Journal of Applied Polymer Science

Synthesis, characterization, and properties of cashew gum graft poly(acrylamide)/magnetite nanocomposites

M. T. Ramesan, K. Surya
Department of Chemistry, University of Calicut, Calicut University P.O., Malappuram, Kerala 673 635, India
Correspondence to: M. T. Ramesan (E-mail: mtramesan@uoc.ac.in)

ABSTRACT: Graft copolymer nanocomposites based on cashew gum and poly(acrylamide) with different concentrations of nano-iron-oxide particles (Fe_3O_4) have been prepared by an in situ polymerization method. The characterization of graft copolymer composite was carried out by FTIR, UV, XRD, SEM, DSC, and TGA, electrical conductivity, and magnetic property [vibrational sample magnetometer (VSM)] measurements. The shift in the spectrum of UV and FTIR peaks shows the intermolecular interaction between metal oxide nanoparticles and the graft copolymer system. The spherically shaped particles observed from the SEM images clearly indicating the uniform dispersion of nanoparticles within the graft copolymer chain. The XRD studies revealed that the amorphous nature of the graft copolymer decreases by the addition of Fe_3O_4 nanoparticles. The glass transition temperature studied from DSC increases with increase in concentration of metal oxide nanoparticles. Thermal stability of composite was higher than the pure graft copolymer and thermal stability increases with increase in content of nanoparticles. Electrical properties such as AC conductivity and dielectric properties of the composites increased with increase in concentration of metal oxide nanoparticles. The magnetic property of graft copolymer nanocomposites shows ferromagnetic and supermagnetism and the saturation of magnetism linearly increased with increasing the Fe_3O_4 content in the polymer composite. © 2016 Wiley Periodicals, Inc. J. Appl. Polym. Sci. **2016**, *133*, 43496.

KEYWORDS: biopolymers and renewable polymers; dielectric properties; differential scanning calorimetry; synthesis and processing; thermogravimetric analysis

Received 1 October 2015; accepted 31 January 2016
DOI: 10.1002/app.43496

INTRODUCTION

Biopolymers obtained from renewable resources have been the center of public interest by virtue of their unique environmental and commercial advantages. The most common natural polymers are starch, cellulose, and chitosan, which were intensely researched alone or combined with synthetic polymers or with inorganic particles to get fully or partially biodegradable material.[1–4] These polymers are suitable in many commodities and in various applications such as surgical implants, artificial sensors drug delivery system, and biomedical engineering. However, these natural polymers have poor properties in modern industrial applications because of their bounded mass in a structure, rheology, and thermal stability and so on. Various biocomposite materials have been developed in recent years due to more environmentally aware consumers, increased price of crude oil, and global warming.[5,6] Different methods have been adopted to modify the structural, morphological, and rheological properties of biopolymers to improve their thermal, mechanical, and electrical properties.

Cashew gum (CG) is particularly an interesting water-soluble polymer exudated from the cashew tree, very abundant in India. It is similar to arabic gum family which is widely used in food industry.[7,8] CG is an acidic polysaccharide complex that contains galactose in the main chain with terminal branches such as glucuronic acid, arabinose, rhamnose, xylose, glucose, and mannose.[9] In the last few years, CG is used as a super adsorber as hydrogel for soil conditions and in drug delivery system.[10,11] Natural gum can play an important role in polymer composite because of their ability to form intermolecular interaction with other polar polymers or filler particles. The polymer composites based on CG have not yet been adequately explored.

Nanocomposites with organic and inorganic hybrids are the special class of materials which sparked enormous interest in the last two decades because these materials exhibit unique and extraordinary properties and it can be applied in diverse areas. The property of these hybrid materials could be controlled through the proper functional group in the polymer or the size, shape, and polarity of the filler particles which result in good mechanical, optical, and electrical properties.[12,13] However, these properties of composites depend on the phase morphology of the new polymer matrix and the interfacial interactions between nanoparticles and the polymer. Research in the field of such

polymer mainly focused on the modification of existing polymers, so that their visibility can further be improved. One of the successful approaches has been preparing the composite polymer network containing different metal oxide nanoparticles such as Fe_3O_4, $MnWO_4$, TiO_2, and fly ash composites.[14–16] Among these, magnetite (Fe_3O_4)-based polymer composites have attracted considerable attention especially in the field of polymer chemistry and physics because of their various applications such as magnetic recording media, photonic crystallites, sensors, and actuators. It has been commonly recognized that the dispersion of nanoparticles into a polymer matrix depends on the size, shape, and polarity of nanofillers.[17] Moreover, the uniform distribution of nanoparticles into a polymer may not be easily achieved by the addition of premade nanosized particles, due to the easy agglomeration of particles inside the polymer chain. This can be overcome by the simple in situ polymerization of nanoparticles with monomers or polymer. Therefore, this work focused on the fabrication of multifunctional nanocomposites by a simple, inexpensive in situ graft copolymerization of metal oxide nanoparticles with acrylamide monomer and CG in an aqueous medium. To synthesize these composites, Fe_3O_4 nanoparticles are dispersed in the aqueous solution of CG by ultrasonication process, followed by the addition of acrylamide with an oxidant in the same solution. The effects of different concentration of magnetite nanoparticles on electrical and magnetic properties are discussed on the basis of structural characterizations like FTIR, UV, XRD, SEM, TGA, and DSC.

EXPERIMENTAL

Materials and Methods

CG was collected from the native trees in Calicut University campus. The gum was purified by dissolving in distilled water at room temperature, filtered, and precipitated from ethyl alcohol. The pure CG was dried and ground in an analytical mill and passed through 90 μm mesh to get fine powder. Sodium dodecylsulfate (SDS), potassium persulphate (KPS), ferrous chloride, ferric chloride, ammonia, methanol, and ethanol were supplied by Merck India and were used without further purification. Distilled water was used in all the experiments.

Synthesis of Magnetite Nanoparticles

The magnetite nanoparticles with 32 nm size were prepared by chemical coprecipitation technique.[18] Ferrous and ferric chloride (2:1 molar ratio) was dissolved in deionized water in an RB flask equipped with condenser. This solution was then stirred for 30 min in an inert atmosphere. Ammonia solution was added to this mixture and regulates the PH up to 11. The reaction was continued for 6 h at 50 °C. The product was cooled in an ice bath and centrifuged at 3000 rpm to collect a black precipitate. It was washed with deionized water to remove excess ion and finally washed with ethanol and dried at 60 °C for 24 h.

Synthesis of CG Graft Poly(Acrylamide)

The synthesis of CG graft poly(acrylamide) (CG-g-PAM) was carried out in an inert atmosphere using KPS as initiator, according to the method suggested by Singh *et al.*[19] The synthetic procedure used for preparation of graft copolymer is 1:0.6 ratio of CG and acrylamide. The required amount of grafted copolymer was prepared by dissolving CG in distilled water in a 250 mL R.B. flask. It was then mixed with 0.1 g KPS, and the mixture was stirred to achieve a clear viscous solution. Then the flask was purged with nitrogen while the temperature was brought to 60 °C. The acrylamide monomer was added into the flask and the reaction was performed for 3 h under continuous stirring. At the end of the polymerization, the reaction mixture was poured into excess amount of acetone and precipitated copolymer were filtered and washed with 30% methanol to remove the homopolymers of poly(acrylamide) (PAM). The product was washed repeatedly with distilled water and dried at 50 °C. The aforementioned method is used for the polymerization of acrylamide in the absence of CG. The samples were stored in a desiccator until further use.

Synthesis of Graft Copolymer/Fe_3O_4 Nanocomposites

A CG-g-PAM/magnetite (Fe_3O_4) nanocomposite was carried out in a 500 mL RB flask under an oxygen-free nitrogen atmosphere. Magnetite nanoparticles (3, 5, 10, and 15 wt %) were mixed with SDS in distilled water and ultrasonicated for 10 min. To this, aqueous solution of CG and acrylamide monomer was added and again ultrasonicated for a period of 20 min. Then 0.1 g KPS was added into the reaction mixture and stirred for 3 h at 60 °C. After the reaction was finished, the graft copolymer composite was coagulated with 10-fold excess of acetone. The product was separated and the homopolymer PAM was removed by washing several times with warm water, until the extract gave no precipitation with methanol. The graft copolymer composite was washed with distilled water and dried to constant weight.

Characterizations

The IR spectra of copolymer composites were recorded on a JASCO (model 4100) Fourier transform infrared spectrophotometer in the region of 4000–400 cm^{-1}. The ultraviolet–visible (UV–vis) absorption spectra of graft copolymer and copolymer containing magnetite composites in water were recorded on a Hitachi U-3000 spectrophotometer. The surface structures of composites were investigated using Field Emission Scanning Electron Microscopy (FESCA)—Hitachi, SU 6600 FESEM). The X-ray diffraction pattern of the sample was recorded on a Bruker AXS D X-ray diffractometer using CuK_α radiation ($\lambda = 1.5406$ Å) with an accelerating voltage of 30 kV. DSC studies were carried out on a V2 6D TA instrument model DSC 2010. Initial scans were taken from 50 to 100 °C to remove the thermal history effects and then cooled to room temperature. Thermal stability of the composites was investigated by a Perkin Elmer thermogravimetric analyzer (TGA) at a heating rate of 10 °C min^{-1}. The prepared samples were finely powered and made into pellet using a hydraulic press. The capacitance and dielectric loss in a frequency range 100–10^6 Hz were found out using Hewlett–Packard LCR Meter. The dielectric constant or relative permittivity (ε_r) of the material was calculated by using the expression:

$$\varepsilon_r = \frac{(C \times d)}{\varepsilon_0 A} \quad (1)$$

where d is the thickness of the sample, C is the capacitance, ε_0 is the permittivity of free space, and A is the area of cross-section of the sample.

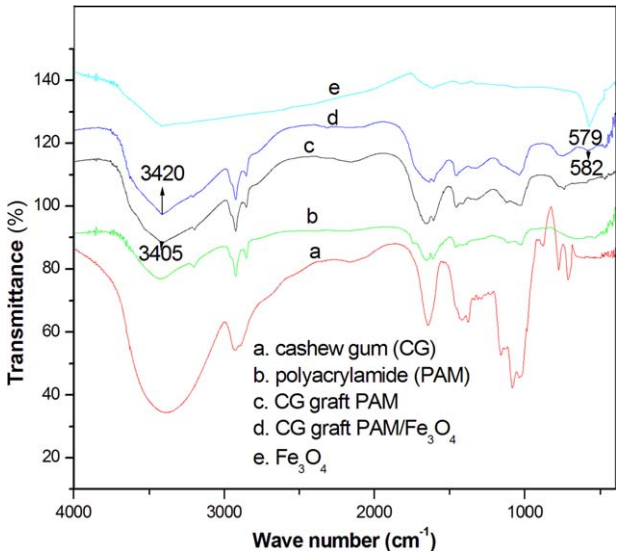

Figure 1. FTIR spectrum of cashew gum, polyacrylamide, cashew tree gum–g-poly(acrylamide), magnetite, and graft copolymer with magnetite nanoparticles. [Color figure can be viewed in the online issue, which is available at wileyonlinelibrary.com.]

The conductivity (σ) of these pellets was measured using the following equation:

$$\sigma_{a.c} = \omega \tan \delta \, \varepsilon_0 \varepsilon_r \quad (2)$$

where $\omega = 2\pi f$, tan δ is the dielectric loss, ε_0 is the permittivity of free space, and ε_r is the relative permittivity of the material. The magnetic properties of the graft copolymer with different content of magnetite nanoparticles were measured using a vibrational sample magnetometer (VSM model LDJ 9600) at room temperatures.

RESULTS AND DISCUSSION

FTIR Characterization

The infrared spectra of CG, PAM, CG-g-PAM, iron oxide nanoparticles, and iron oxide nanoparticles incorporated graft copolymer are shown in Figure 1. The absorption band derived from magnetite nanoparticles [Figure 1(e)] observed at 579 cm^{-1} is the typical stretching vibration band of Fe—O bond. The IR spectra of CG [Figure 1(a)] display a broad band at 3414 cm^{-1}, which is the OH stretching vibration. The IR band located at 2930 cm^{-1} is attributed to the stretching of CH group and the strong signal appeared at 1648 cm^{-1} is due to the OH scissor vibration from bonded water molecules.[20] The absorption peak appeared at 1420 cm^{-1} is related to the angular deformation of CH_3 group of polysaccharide. The peaks obtained at 1160, 1086, and 1028 cm^{-1} are owing to the stretching vibrations of C—O—C from the glucosidic bonds and OH absorption from alcohol. PAM [Figure 1(b)] shows the bands at 3440 cm^{-1} and shoulder at 3201 cm^{-1} are associated with the asymmetrical and symmetrical stretching of NH bond, respectively. The band appeared at 2928 cm^{-1} is the typical stretching of CH bonds. The IR bands located at 1658 cm^{-1} and 1610 cm^{-1} are the stretching of C=C group of typical amide I and the angular deformity of NH_2 group of amide II, respectively.[21] The absorption at 1455 cm^{-1} is attributed to the CN bond stretching. Spectrum of graft copolymer [Figure 1(c)] shows the characteristic absorption band of CG and the acrylamide with some slight shift in the position of peaks. The broad band appeared at 3405 cm^{-1} is attributed to the overlapping of OH and NH indicating grafting of acrylamide onto CG. From the IR spectra of graft copolymer nanocomposite [Figure 1(d)], it can be seen that the in situ polymerization magnetite with CG and acrylamide induces a new absorption at 582 cm^{-1} (typical stretching of Fe—O bond) along with shift in the OH and NH group of graft copolymer (i.e., from 3405 to 3420 cm^{-1}), which may be due to the strong intermolecular interaction between the polar groups of graft polymer with the polar group of graft copolymer metal oxide nanoparticles. These interactions clearly indicated that the graft copolymer chains are encapsulated on the surface of magnetite nanoparticles.

UV Spectra of CG-g-PAM/Fe_3O_4

The UV–vis absorption spectra of CG, PAM, CG-g-PAM, and magnetite nanoparticle incorporated CG-g-PAM are shown in Figure 2. The π–π^* and n–n* transitions of CG, PAM, and CG-g-PAM are appeared at 217 and 299 nm for CG, 237 and 293 nm for PAM, and 230 and 282 nm for CG-g-PAM, respectively. However, the corresponding π–π^* and n–n* transitions of graft copolymer/Fe_3O_4 nanocomposite is appeared at 251 and 318 nm. It is well clear from the figure that absorbance values of the composites are shifted to higher wavelength region with respect to that of CG, PAM, and graft copolymer. This shift in absorption peak is attributed to the strong intermolecular interaction between the metal oxide nanoparticles and the polar segments of graft copolymer. The broadness of absorption peak indicates the complexation of nanoparticles and the shift in peaks reveals the decrease in amorphous nature of the materials.[22]

Scanning Electron Microscopy (SEM)

To demonstrate the above statement, morphology of CG-g-PAM nanocomposites with different content of Fe_3O_4 nanoparticles is

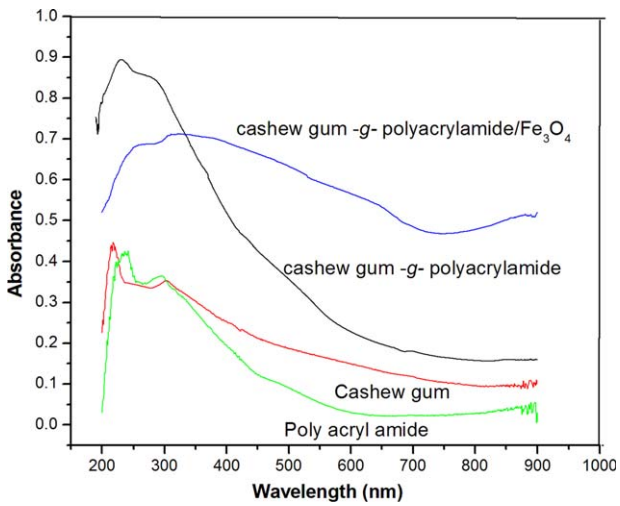

Figure 2. UV spectra of cashew gum, polyacrylamide, cashew gum–g-poly (acrylamide), and graft copolymer with magnetite nanoparticles. [Color figure can be viewed in the online issue, which is available at wileyonlinelibrary.com.]

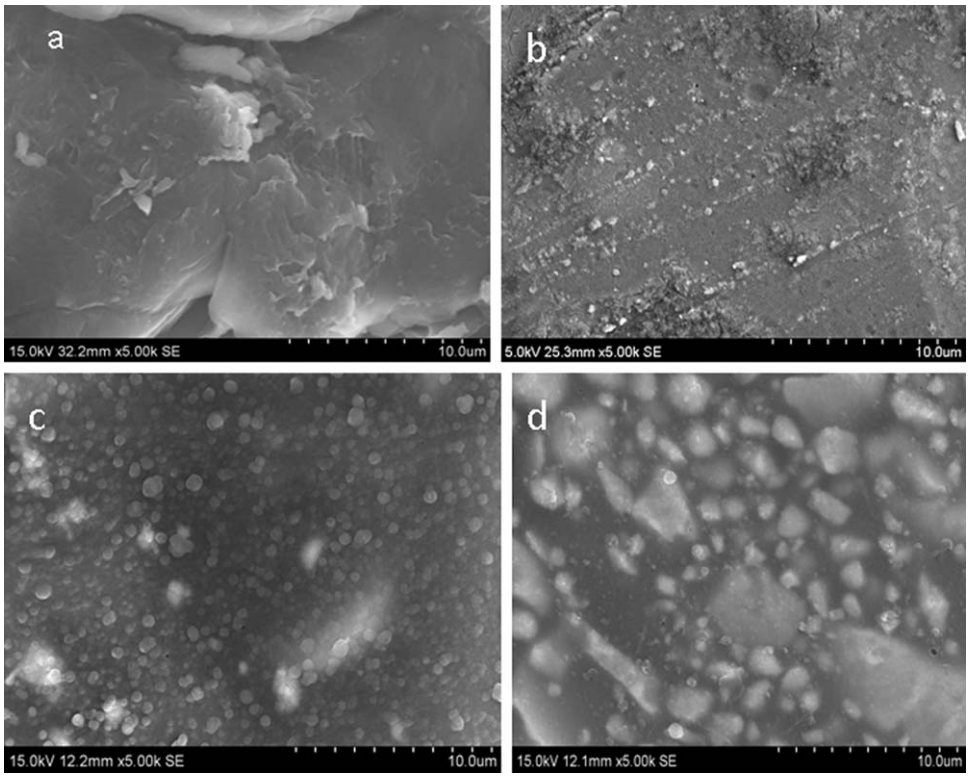

Figure 3. SEM images of (a) CG-g-PAM, (b) CG-g-PAM/5 wt % Fe_3O_4, (c) CG-g-PAM/10 wt % Fe_3O_4, (d) CG-g-PAM/15 wt % Fe_3O_4.

investigated by SEM and it is given in Figure 3. The SEM image of graft copolymer [Figure 3(a)] exhibits a uniformly processed structure with a homogeneous composition. Figure 3(b) represents the morphology of graft copolymer/5 wt % Fe_3O_4 nanocomposite indicates a good dispersion of nanoparticles into the copolymer chain. As the concentration of nanoparticles increased to 10 wt % [Figure 3(c)], it can be seen that magnetite nanoparticles are well inserted into the macromolecular chain of copolymer, having spherically shaped particles with good uniformity and adhesiveness. The uniform dispersion of metal oxide nanoparticles is due to the electronic rearrangements in Fe_3O_4 particles based on the co-ordination interaction between the copolymer segments with the Fe_3O_4 nanoparticles. However, in the case of higher concentration of nanoparticles [Figure 3(d)], the morphology of the composite is changed and the metal nanoparticles are slightly elongated which is due to the greater stress developed in the polymer nanocomposite.

X-ray Diffraction Pattern (XRD)

Figure 4 shows the XRD patterns of Fe_3O_4, CG-g-PAM, and graft copolymer with 10 wt % of Fe_3O_4. The XRD profile of the synthesized Fe_3O_4 nanoparticles shows four diffraction peaks at $2\theta = 35.3°$, 41.8°, 56.9°, 62.3°, which correspond to the 311, 400, 511, and 440 crystal plane reflection[23] of pure Fe_3O_4. CG graft copolymer shows a broad diffraction peak at $2\theta = 20.6°$, indicating the amorphous nature of the copolymer. The XRD patterns of CG-g-PAM/Fe_3O_4 is found to keep the diffraction characteristics of copolymer and Fe_3O_4 nanoparticles, revealing that additional crystalline order has been introduced into the nanocomposite. In general, when a polymer contains large crystalline region and then higher the degree of regularity in arrangement or ordering of polymer chain, higher is the crystallinity.[24] It is also clear from the figure that the broad amorphous diffraction peak of graft copolymer composite is reduced and shifted to higher angle (i.e., from $2\theta = 20.6°$ to 21.56°) with respect to pure graft copolymer. The shift in diffraction peak is due to the change in interlayer volume by the insertion of magnetite nanoparticles into the graft copolymer chains. The increase in degree of crystallinity with the encapsulation of magnetite particles is due to the intermolecular interaction between the polar groups of metal oxide nanoparticles with the

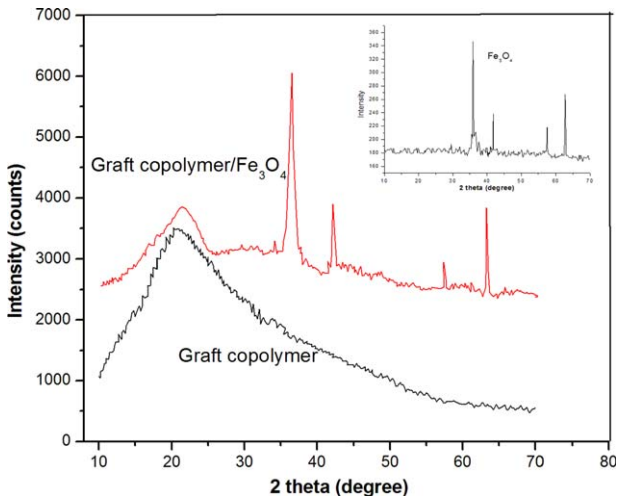

Figure 4. XRD patterns of Fe_3O_4, cashew gum–g-poly(acrylamide), and graft copolymer with 10 wt % of magnetite nanoparticles. [Color figure can be viewed in the online issue, which is available at wileyonlinelibrary.com.]

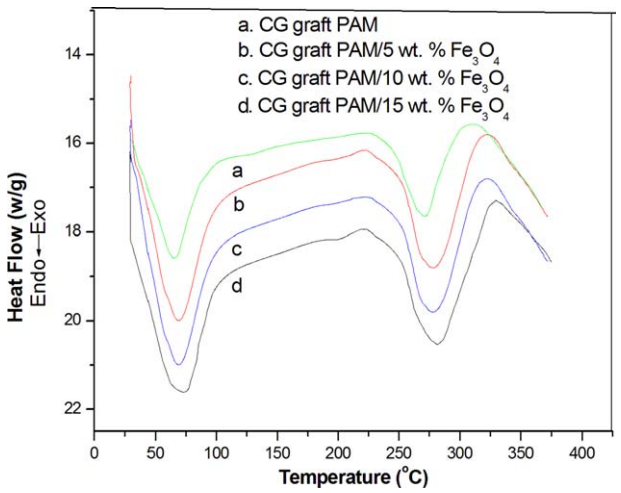

Figure 5. DSC thermograms of cashew gum–g-poly(acrylamide) copolymer with various concentrations of magnetite nanoparticles. [Color figure can be viewed in the online issue, which is available at wileyonlinelibrary.com.]

polar group of graft copolymer, which leads to a highly ordered structure in the polymer matrix. This result has been further confirmed from DSC study.

Differential Scanning Calorimetry (DSC)

The thermal transition of CG-g-PAM and the graft polymer with different contents of magnetite nanoparticles were studied by DSC in the temperature range 30–375 °C and are given in Figure 5. The DSC curve of pure graft copolymer showed broad endothermic peaks at 65.4 °C and 271 °C, which are the glass transition (T_g) and melting temperature T_m of the graft polymer, respectively. It is observed from the figure that the glass transition temperature and melting behavior of nanocomposites are higher than the graft copolymer and these values increase with increase in concentration of metal oxide nanoparticles. The T_g and T_m values of different concentration of Fe_3O_4 containing graft copolymers are observed at 68.6 °C; 277 °C (5 wt %), 70 °C; 278 °C (10 wt %), and 74 °C; 282 °C (15 wt %), respectively. The increase in T_g and T_m values of composites with the increase in concentration of magnetite nanoparticles is due to more ordered arrangement of metal oxide nanoparticles inside the graft copolymer chain, which result from the intermolecular interaction between the metal oxide particles and the copolymer.[25] Hence it can be concluded that the thermal parameters such as glass transition temperature and melting behavior depend on the concentrations of metal oxide nanoparticles in the graft copolymer.

Thermogravimetric Analysis (TGA)

The thermal degradation behavior of CG-g-PAM and the copolymer containing different weight percentage of Fe_3O_4 nanoparticles is shown in Figure 6. TGA result shows two stages of decomposition patterns for all the compounds. The first stage of weight loss at 225–290 °C is due to the degradation of polysaccharide, ammonia, and the formation of imine.[26] The second stage degradation starts from 300 to 390 °C is ascribed to the decomposition of polymer. The graft copolymer degrades fleetly at a temperature from 50 to 600 °C. The final mass loss is 15 wt % for Fe_3O_4-incorporated graft copolymer at 600 °C and it is higher than that of the pure graft copolymer (final mass loss for 15 wt % Fe_3O_4/graft polymer is 84%, while for pure graft copolymer is 99.8%). The final char residue in TGA is a measure of fame resistance of the polymer composites.[27] Results from this study indicate that the graft copolymer/Fe_3O_4 nanocomposites have good thermal stability and flame resistance than pure graft copolymer. The increase in thermal stability with increase in content of nanoparticles is attributed to the strong intermolecular interaction between metal oxide and the graft copolymer. Thus, TGA result is in good agreement with the XRD and DSC measurements.

AC Conductivity

The AC electrical properties of various concentrations of magnetite nanoparticles-encapsulated CG-g-PAM composites are analyzed as a function of frequency and are illustrated in Figure 7. From the graphs, it can be inferred that the conductivity of nanocomposites is much higher than the pure graft copolymer and the conductivity of composites increases with increase in concentration of nanoparticles. Furthermore, the conductivity of all the composites increases with increase in frequency indicating the formation of charge carriers. In pure graft copolymer, the macromolecular chains are randomly oriented (which is well clear from the amorphous region of polymer from XRD measurement), and hence the linkage among the polymer chain is very poor resulting in relatively lower electrical conductivity.[28] However, the interfacial interaction between the metal oxide nanoparticles with the copolymer leads to regularity in the chain which helps to acquire compactness of the composite materials. Hence these interactions strengthen the coupling through grains that result in an enhanced conductivity in CG-g-PAM/Fe_3O_4 composite as compared to bare polymer. In addition, the uniform distribution of nanoparticles to the polymer matrix leads to increased conductivity values. Such a uniform dispersion of nanoparticles is an indication of particle–particle interfaces, which leads to overall percolation conductivity. The conduction in polymer composite is taking place through the

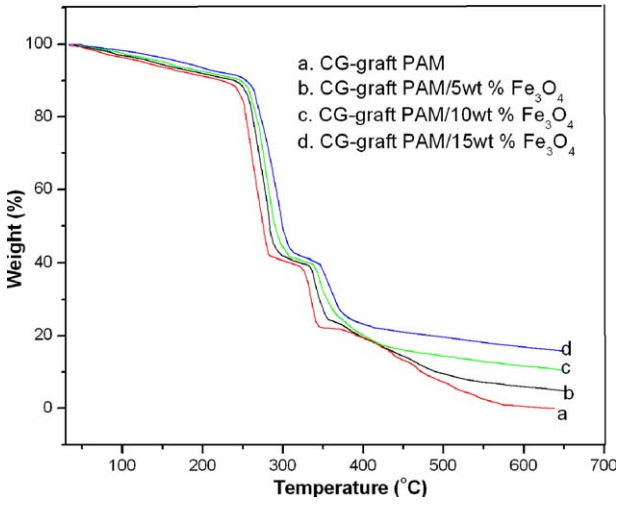

Figure 6. TGA curves of graft copolymer with different concentrations of Fe_3O_4. [Color figure can be viewed in the online issue, which is available at wileyonlinelibrary.com.]

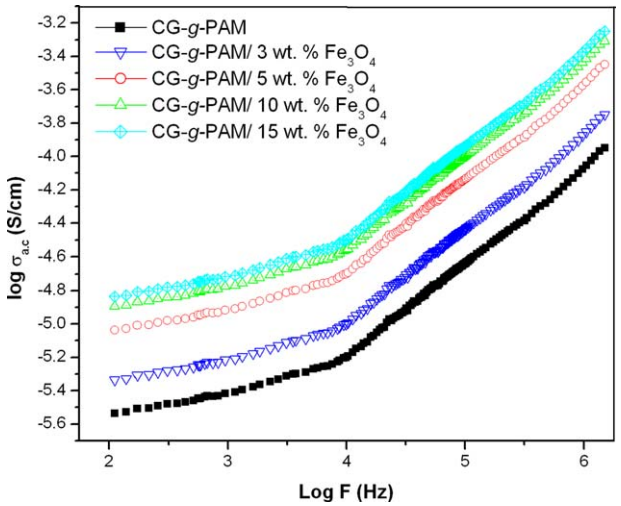

Figure 7. Variation of AC conductivity of cashew gum–g-poly(acrylamide) copolymer with various concentrations of magnetite nanoparticles. [Color figure can be viewed in the online issue, which is available at wileyonlinelibrary.com.]

electronic delocalization via the crystalline domains of nanoparticles which are surrounded by the amorphous region of polymer chain. It is also clear from the figure that the magnitude of increase in conductivity with increasing the loading of nanoparticles is steeply up to 10 wt % Fe_3O_4, and thereafter the value slowly increases. At higher loading of Fe_3O_4, the individual nanoparticles combine to form strong aggregates and these aggregates are loosely bounded to form internal voids and crannies in the composite, which affect the conductivity values of 15 wt % of Fe_3O_4 compound with respect to 10 wt % of composite. These results are in good agreement with the SEM analysis.

Dielectric Constant (ε_r)

The plots of dielectric constant (ε_r) versus log frequency at room temperature for CG-g-PAM and CG-g-PAM/Fe_3O_4 nanocomposites are given in Figure 8. The dielectric constant initially decreases steeply with increasing frequency and the dielectric value became constant around 10^4 Hz. The decrease in dielectric constant with increase in frequency is due to the lag of hopping frequency electrons between the Fe atom and the polar segment of graft copolymer and that creates bilayer polarization.[29] This type of polarization influences the low-frequency dielectric constant. From the figure, it can be seen that the dielectric constant of composites are much higher than the bare polymer and the dielectric values increases with increase in content of nanoparticles. The dielectric constant of polymer composite depends upon interfacial interaction, ionic, electronic, dipolar, and space charge polarization. Among these polarizations, the space charge contribution depends on the method of preparation, purity of compounds, and the perfection of polymer matrix. In this study, copolymers having different content of iron oxide nanoparticles are synthesized by an in situ method, which leads to the polymerization of CG and acrylamide monomer on the surface of metal oxide nanoparticles. The addition of metal oxide particles induces some defects in the polymer matrix that significantly influences the space charge polarization. The dispersion of nanoparticles also plays an important role in the higher values of the composites. The in situ polymerization leads to uniform distribution of fillers in the polymer (better revealed from SEM analysis), where the metal oxide particles are in physical contact or very close to each other. Due to this close packing of nanoparticles, the dipole–dipole interactions are very high and hence greater will be the polarization. The dielectric behavior of these composites can be used for various applications such as in conductive paints, sensors, and so on.

Dielectric Loss (tan δ)

The dielectric loss tangent (tan δ) versus log frequency at room temperature of CG-g-PAM with various content of Fe_3O_4 nanoparticles are presented in Figure 9. The tan δ is the direct

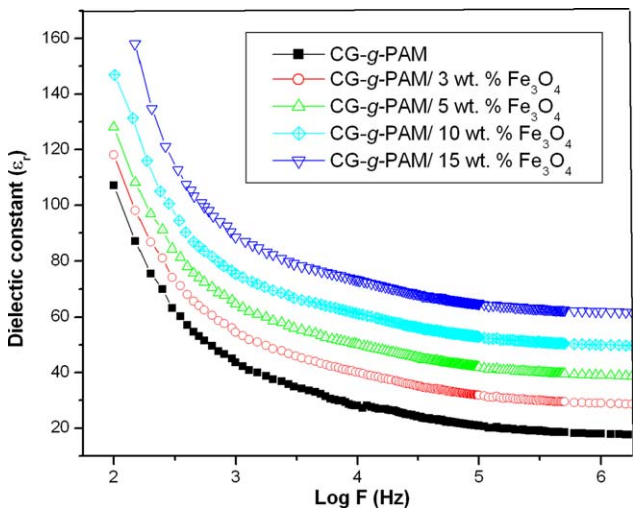

Figure 8. Frequency dependence of dielectric constant of cashew gum–g-poly(acrylamide) copolymer with different concentrations of magnetite nanoparticles. [Color figure can be viewed in the online issue, which is available at wileyonlinelibrary.com.]

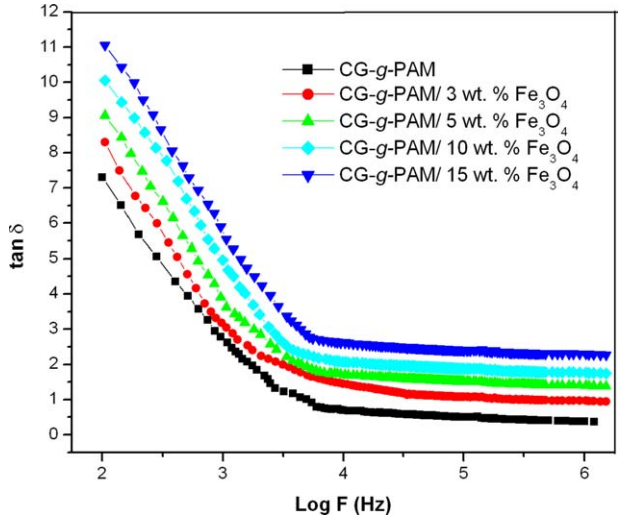

Figure 9. Dielectric loss versus frequency plots for cashew gum–g-poly (acrylamide) copolymer with various content of magnetite nanoparticles. [Color figure can be viewed in the online issue, which is available at wileyonlinelibrary.com.]

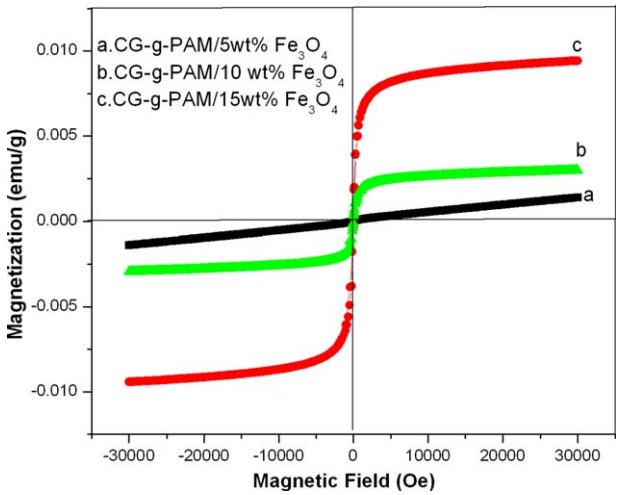

Figure 10. Dependence of applied magnetic field on the saturated magnetization of CG-g-PAM/Fe_3O_4 nanocomposite. [Color figure can be viewed in the online issue, which is available at wileyonlinelibrary.com.]

measure of electrical energy associated with a material. It can be seen that the tan δ values of all the samples decreases rapidly at lower frequencies and slowly at higher frequencies. The high value of dielectric loss tangent at lower frequencies is attributed to the interfacial polarization developed between the graft copolymer and the metal oxide nanoparticles. However, at higher frequencies, the rotational motion of the polar molecules get sufficiently less time to keep up themselves with the applied electrical field in the composite matrix, and hence the tan δ decreases at higher frequencies.[30] The tan δ values of composites are higher than the graft copolymer and the dielectric loss tangent increases with increase in concentration of nanoparticles. The high-value tan δ is due to the relaxation process originated from the local motion of polar groups present in the polymer and the metal oxide particles. Further, the incorporation of nanoparticles to the polymer affects the viscosity of the polymer matrix and that leads to an increase in tan δ values. Moreover, the progressive addition of conductive iron oxide nanoparticles into an insulating CG-g-PAM leads to the development of conductive aggregates, which in turn increases the dielectric loss tangent with an increase in concentration of nanoparticles.

Magnetic Properties by VSM Analysis

The magnetization curve of CG-g-PAM copolymer/Fe_3O_4 nanocomposite with the applied field at room temperatures is displayed in Figure 10. From the figure, it can be seen that the composites with 10 and 15 wt % of magnetite nanoparticles have hysteresis loops, which indicates that the nanocomposite exhibits ferromagnetic and superparamagnetic behavior. The magnetic properties of fabricated nanocomposites strongly depend on the amount of dispersed Fe_3O_4 nanoparticles, and in this work, the saturation of magnetization (M_s) of the composite exhibits monotone increase with the magnetite content in graft copolymer matrix. It can be observed that the concentration of magnetite nanoparticles increases from 5 to 15 wt %, the M_s value of nanocomposite is found to be 0.0016 emu/g (electromagnetic unit per gram) to 0.0097 emu/g, respectively. Therefore, the fabricated CG-g-PAM copolymer/Fe_3O_4 composite can be used as electrical and magnetic shielding materials because they have a wide range of electrical conductivity as well as saturation magnetization.[31]

CONCLUSIONS

The functional properties of CG-g-PAM copolymer were successfully improved by the addition of magnetite nanoparticle by a simple in situ polymerization technique. FTIR and UV studies revealed the interaction between Fe_3O_4 nanoparticles and the graft copolymer. The morphological observations indicated that the nanoparticles were uniformly distributed within the macromolecular chain of graft copolymer with spherically shaped particles and the dispersion of nanoparticles decreases with increase in concentration of Fe_3O_4. The crystal structure study suggests that the encapsulation of magnetite by the copolymer, which impart a uniform arrangement of nanoparticles in the polymer matrix. DSC results indicated that the glass transition temperature of the nanocomposite was higher than the graft copolymer and the glass transition temperature increases with increase in content of nanoparticles. An increase in thermal stability of nanocomposite with increase in concentration of metal oxide particles was observed from the TGA plots, which is due to the strong intermolecular interaction between the nanoparticles and the copolymer chain. The higher conductivity of nanocomposite than the graft polymer is due to the interfacial interaction of magnetite nanoparticles with the copolymer, which leads to an enhanced regularity of chain in the composites. Dielectric constant and dielectric loss tangent of composites were significantly improved with increase in content of metal oxide nanoparticles, attributed to the local displacement of electrons that induces polarization in the graft copolymer composite. Magnetic properties analyzed by vibrating sample magnetometer (VSM) indicated that the electromagnetism of copolymer/Fe_3O_4 nanocomposites were superparamagnetic in nature. The high values of electrical, thermal, and magnetic properties of the nanocomposite suggested a possible application of the fabricated CG graft copolymer/magnetite materials in the field of sensors, actuators, and magnetic shielding materials.

REFERENCES

1. Klemm, D.; Heublein, B.; Fink, H. P.; Bohn, A. *Angew. Chem. Int. Ed.* **2005**, *44*, 3358.
2. Hu, X.; Cebe, P.; Weiss, A. S.; Omenetto, F.; Kaplan, D. L. *Mater. Today* **2012**, *15*, 2018.
3. Appelqvist, I. A. M.; Debet, M. R. M. *Food Rev. Int.* **1997**, *13*, 163.
4. Sareena, C.; Sreejith, M. P.; Ramesan, M. T.; Purushothaman, E. *J. Reinf. Plast. Compos.* **2014**, *33*, 412.
5. Kluver, E.; Meyer, M. *J. Appl. Polym. Sci.* **2013**, *128*, 4201.
6. Ramesan, M. T. *Pet. Sci. Technol.* **2014**, *32*, 1775.
7. dePaula, R. C. M.; Heatley, F.; Budd, P. M. *Polym. Int.* **1998**, *45*, 27.

8. Chowdhury, P.; Samui, S.; Kundu, T.; Saha, B. *J. Chin. Chem. Soc.* **2004**, *51*, 97.
9. daSilva, D. A.; Feitosa, J. P. A.; Paula, H. C. B.; dePaula, R. C. M. *Mater. Sci. Eng. C* **2009**, *29*, 437.
10. Guilherme, M. R.; Reis, A. V.; Takahaschi, S. H.; Rubira, A. F.; Feitosa, J. P. A.; Muniz, E. C. *Carbohydr. Polym.* **2005**, *61*, 464.
11. Maciel, J. S.; Silva, D. A.; dePaula, H. C. B.; dePaula, R. C. M. *Eur. Polym. J.* **2005**, *41*, 2726.
12. Hrehorova, E.; Bliznyuk, V. N.; Pud, A. A.; Shevchenko, V. V.; Fatyeyeva, K. Y. *Polymer* **2007**, *48*, 4429.
13. Najar, M. H.; Majid, K. *J. Mater. Sci. Mater. Electron.* **2013**, *24*, 4332.
14. Ramesan, M. T. *Adv. Polym. Tech.* **2013**, *32*, 928.
15. Radoicic, M.; Saponjic, Z.; Marjanovic, G. C.; Konstantinovic, Z.; Mitric, M.; Nedeljkovic, J. *Polym. Compos.* **2012**, *33*, 1482.
16. Ramesan, M. T. *J. Thermoplast. Comp. Mater.* **2015**, *28*, 1286.
17. Ramesan, M. T. *Polym. Compos.* **2012**, *33*, 2169.
18. Ramesan, M. T. *Int. J. Polym. Mater. Polym. Biomater.* **2013**, *62*, 277.
19. Singh, V.; Tiwari, A.; Tripathi, D. N.; Sanghi, R. *Carbohydr. Polym.* **2004**, *58*, 1.
20. Srivastava, A.; Tripathy, J.; Mishra, M. M.; Behari, K. *J. Appl. Polym. Sci.* **2007**, *106*, 1353.
21. Adhikary, P.; Singh, R. P. *J. Appl. Polym. Sci.* **2004**, *94*, 1411.
22. Tavares, A.; Arruda, B. C.; Boes, E. S.; Stefani, V.; Stassen, H. K.; Campo, L. F.; Bechtold, I. H.; Merlo, A. *J. Braz. Chem. Soc.* **2012**, *23*, 880.
23. Jayakrishnan, P.; Ramesan, M. T. *AIP Conf. Proc.* **2014**, *1620*, 165.
24. Ramesan, M. T.; Jasna, V. C.; Francis, J.; Abdu, R. V. P.; Subburaj, M. *Chemist* **2015**, *88*, 1.
25. Shariatzadeh, B.; Moradi, O. *Polym. Compos.* **2014**, *35*, 2050.
26. Nayak, B. R.; Singh, R. P. *J. Appl. Polym. Sci.* **2001**, *81*, 1776.
27. Anilkumar, T.; Ramesan, M. T. *AIP Conf. Proc.* **2014**, *1620*, 28.
28. Huang, C.; Zhang, Q. M.; deBotton, G.; Bhattacharya, K. *Appl. Phys. Lett.* **2004**, *84*, 4391.
29. Bengoechea, M. R.; Aliev, F. M.; Pinto, N. J. *J. Phys. Cond. Matter* **2002**, *14*, 11769.
30. Ramesan, M. T. *Polym. Eng. Sci.* **2014**, *54*, 438.
31. Kong, I.; Ahmad, S. H.; Abdullah, M. H.; Hui, D.; Yusoff, A. N.; Puryanti, D. *J. Magn. Magn. Mater.* **2010**, *322*, 3401.